Geophysical Monitoring Of High-Level Radioactive Waste Repositories

Hansruedi Maurer [1*], Edgar Manukyan [1], Lenka Koskova [2], Milan Hokr [2], Juhani Korkealaakso [3], Edgar Bohner [3], Bruna De Carvalho Faria Lima Lopes [4], Alessandro Tarantino [4]

[1]ETH Zurich, Sonneggstrasse 5, Zürich, Switzerland

[2]University of Liberec, Studentská 1402/2, 461 17 Liberec, Czech Republic

[3]VTT Technical Research Center of Finlang LTD, P.O. Box 1000, FI-02044 VTT, Finland

[4]University of Strathclyde, 75 Montrose Street, G1 1XJ, Glasgow, U.K.

* Corresponding Author, E-mail: (hansruedi.maurer@erdw.ethz.ch)

Summary

Non-invasive monitoring of radioactive waste repositories is one of the key objectives addressed in the MODERN2020 project. For this task, geophysical techniques offer excellent means. Previous studies have identified seismic full waveform inversion (FWI) to be the most promising option for delineating subtle changes within a repository using data acquired outside of the repository. Significant anisotropy of the host rock, particularly in clay environments, precluded so far application of FWI technology for repository monitoring. With the development of a novel model parameterization, this problem could be resolved. Moreover, incorporation of structural constraints further improved the quality and reliability of our FWI algorithms. This was demonstrated with a field data set acquired in the Mont Terri rock laboratory. For a better characterization of small differential changes between two consecutive experiments, a novel differential tomography methodology was developed. It was tested with field data sets, with which differential traveltime inversions were performed. It is expected that this new method can be transferred in a straightforward manner to FWI problems. FWI technologies require extensive data analyses and substantial computer resources. Therefore, it was checked, if it is possible to employ quick and inexpensive tools, with which temporal changes in a repository can be detected, but not necessarily imaged. For that purpose, an anomaly detection algorithm was developed, and it will be tested with field data. In addition to seismic methods, geoelectrical techniques can provide valuable information for repository monitoring. For that purpose, tomographic algorithms for geoelectrical and induced polarization data were established and tested with laboratory data. For transferring the electrical parameters, obtained from these tomographic inversions, into relevant physical parameters, such as temperature and moisture content, calibration measurements were performed, and constitutive relationships between these parameters were established.

1. Introduction

Geophysical techniques offer powerful means for the implementation of non-invasive monitoring of radioactive waste repositories. The indirect nature of geophysical measurements (i.e., material properties are not measured directly, but through the geophysical data that are affected by the material properties relevant to repository system) allows obtaining information on the repository and it engineered barrier system (EBS) without placing sensors within the regions of interest. However, this can result in considerable uncertainties and ambiguities and more research is required for obtaining meaningful diagnostic information. Extensive reviews of previous work indicated that seismic full waveform inversion (FWI) currently offers the most promising opportunities, but also geoelectrical methods can provide very useful information. Results, obtained so far with these techniques, show that there is a great margin for improvements.

Here, we present results from several studies, in which a variety of geophysical techniques, suitable for high-level radioactive waste repository monitoring, have been employed. In particular, novel FWI and differential tomography techniques, suitable for waveform data, are presented, an anomaly detection algorithm is discussed, and geoelectrical and induced polarization techniques are proposed. Finally, an innovative calibration technique is presented that allows conversions from geophysical quantities to engineering parameters, such as moisture content and temperature.

2. Seismic full waveform inversions (FWI)

In FWI experiments, elastic waves are generated at some distances from the repository. These waves propagate through the repository and are recorded by a seismic acquisition system. Due to interactions between the seismic waves and the repository, the recorded seismograms are influenced by the physical state of the repository. Hence, the seismograms contain information about elastic properties of the repository. This information is used by the FWI algorithm to construct subwavelength resolution images of the elastic properties of the repository.

The unknown physical parameters, influencing the seismic waves, include the elasiticity tensor, and density. Since typical host rocks may exhibit significant anisotropy, several elements of the fourth-order elasticity tensor need to be considered. Recent work has shown (e.g. [1–3]) that an appropriate model parameterization is essential for the success of anisotropic FWI.

Here, a model parameterization was sought that is suitable for crosshole experiments. Extensive testing with synthetic data revealed that a parameterization including four velocity parameters and density is most suitable. More details can be found in [4]. To further improve the reliability of the FWI results, cross-gradient constraints were applied, which enforced structural similarity between the five model parameter types [4].

The novel FWI algorithm was applied to a data set acquired at the Mont Terri URL in the Opalinus Clay in north-west Switzerland. The experiment was focused on the imaging of a 1-m-diameter tunnel and its excavation damage zone (EDZ) (Figure 1). Seismic signals were generated with a high frequency P wave sparker source at every 0.25 m in the lower borehole and recorded with 48 three-component geophones. The geophones were cemented in the upper borehole with 0.5 m spacing between the sensors.
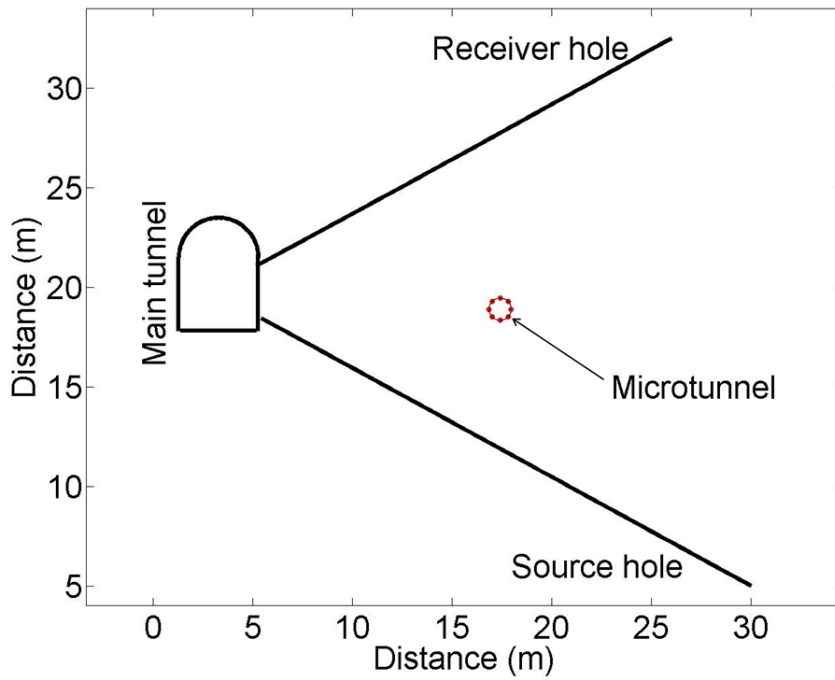
Figure 1. Schematic drawing of the layout of the non-intrusive seismic tomography experiment in the HG-A micro-tunnel at Mont Terri URL.
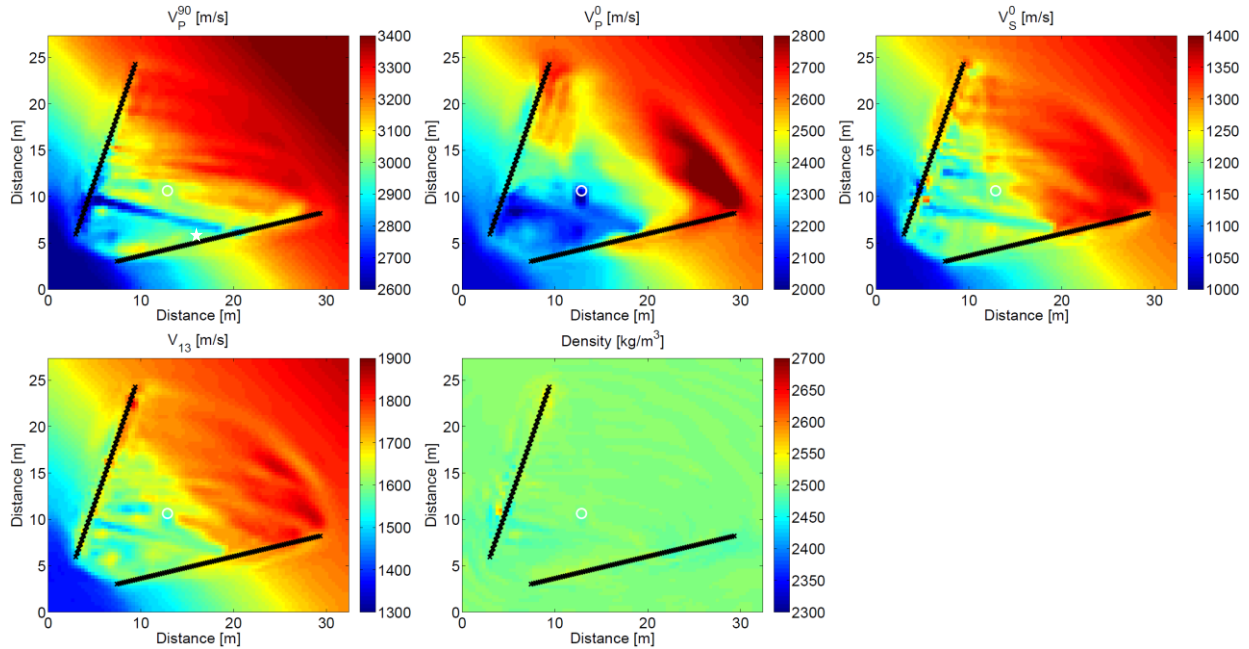

Figure 2. FWI results of data recorded in Mont Terri. The coordinate system is rotated in order to make the direction of symmetry axis vertical. Black crosses indicate locations of sources and receivers. White circles indicate location of the microtunnel.

Figure 2 shows FWI results. Images of the three velocity parameters V_P^{90}, V_S^0 and V_{13} show a clear, 1-2 m wide layer with lower velocities. This layer can be interpreted as a fracture zone also detected by borehole logging [5]. Additionally, reconstruction of V_P^0 shows hints of the microtunnel and its EDZ.

3. Differential tomography with boerehole radar data

Monitoring temporal changes within a volume of interest is one of the primary missions of geophysical surveying, and it finds many applications related with near surface targets, such as groundwater fluctuations (e.g., [6]), freezing and thawing of permafrost (e.g.,[7]), and radioactive waste repository monitoring (e.g., [8]).

The simplest monitoring option is to perform repeated surveys in a consistent manner and to analyze the data sets individually. Temporal changes can then be inferred by qualitative or quantitative comparisons of the results (parallel difference strategy, e.g. [9]). If a tomographic inversion algorithm is involved in the data analysis, the results obtained from a first data set can be used as the initial model for the inversion of the follow-up data set (sequential difference strategy). It is also possible to invert directly for the differences of two data sets. This is referred as the double-difference strategy [9]. This approach is particularly useful (i) in the presence of systematic data errors, and (ii), when the data differences can be determined more accurately and/or more consistently than the actual data.

Double-difference traveltime tomography was applied to a borehole radar data set acquired in the framework of the FE full scale experiment at Mont Terri [10]. Its main objective is to demonstrate that high-level radioactive waste can be stored safely in a deep geological repository. For that purpose, a 3 m diameter tunnel was drilled that should mimic a full-scale repository. High-level radioactive waste canisters are simulated by placing three heaters within the tunnel. After their installation, the tunnel was backfilled with a granulated bentonite mixture (GBM) and finally sealed with a shotcrete plug. The heaters were then switched on, and temperatures reached approx. 130° Celsius on the heater surfaces, and, depending on the position, 45 to 60° at the tunnel walls.

For monitoring temporal changes of the GBM, two fiberglass pipes were inserted prior to the installation of the shotcrete plug. As shown in Figure 3, these pipes extended beyond the first heater in the tunnel. They were employed for a variety of borehole logging surveys and crosshole measurements.
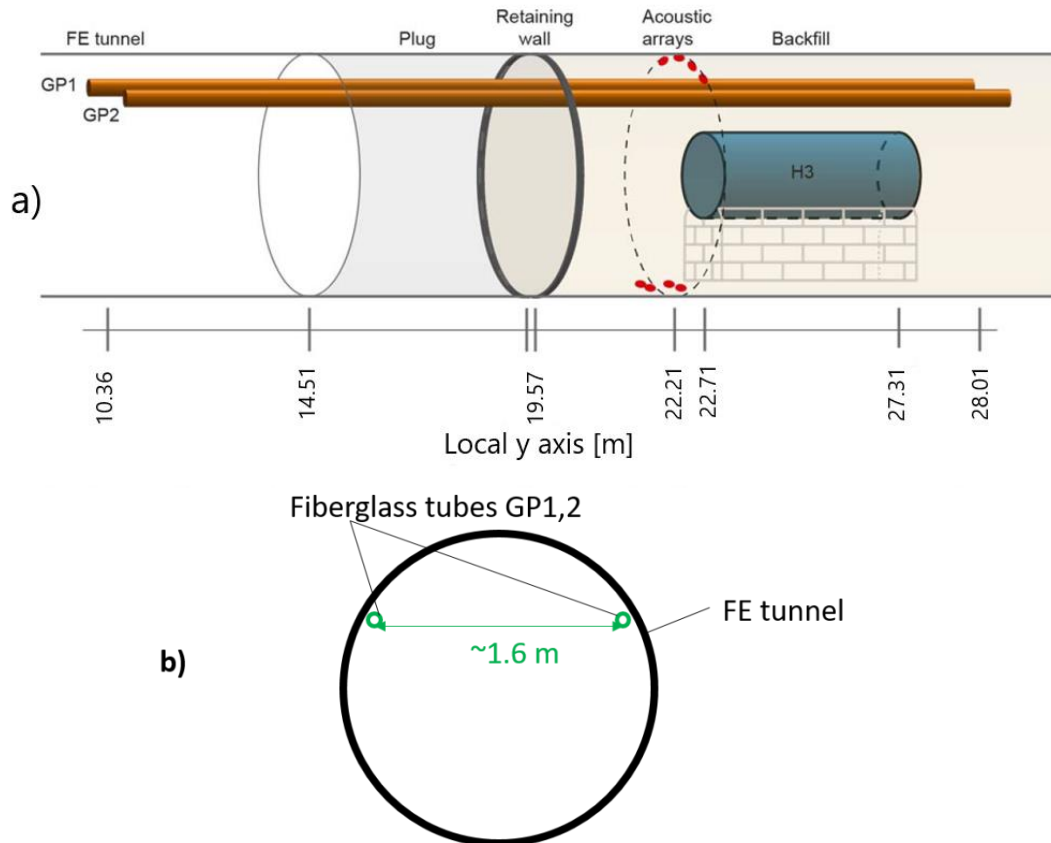
Figure 3. Setup of the FE experiment. a) Side view – GP1 and GP2 are the fiberglass tubes within which the crosshole experiments were performed. H3 represents the heating unit. b) View along the tunnel axis.

Here, we consider crosshole radar measurements performed between GP1 and GP2. Travel-time tomography results are shown in Figure . The left panels show absolute tomograms of the six experiments carried out so far. The first experiment was performed prior to switching on the heater. After switching on the heater, there is a considerable drop of radar propagation velocity in the region of the heater. This is due to the temperature dependency of the dielectric permittivity that governs the radar velocities. At later experiments, we observe the appearance of low- and high-velocity heterogeneities. They can be attributed to the penetration of moisture into the GBM and the formation of air-filled voids.

The right panels in Figure show the results obtained from double-differnce tomography. These images are particularly useful for studying the evolution of the small-scale heterogeneities that appeard in the course of the experiments.
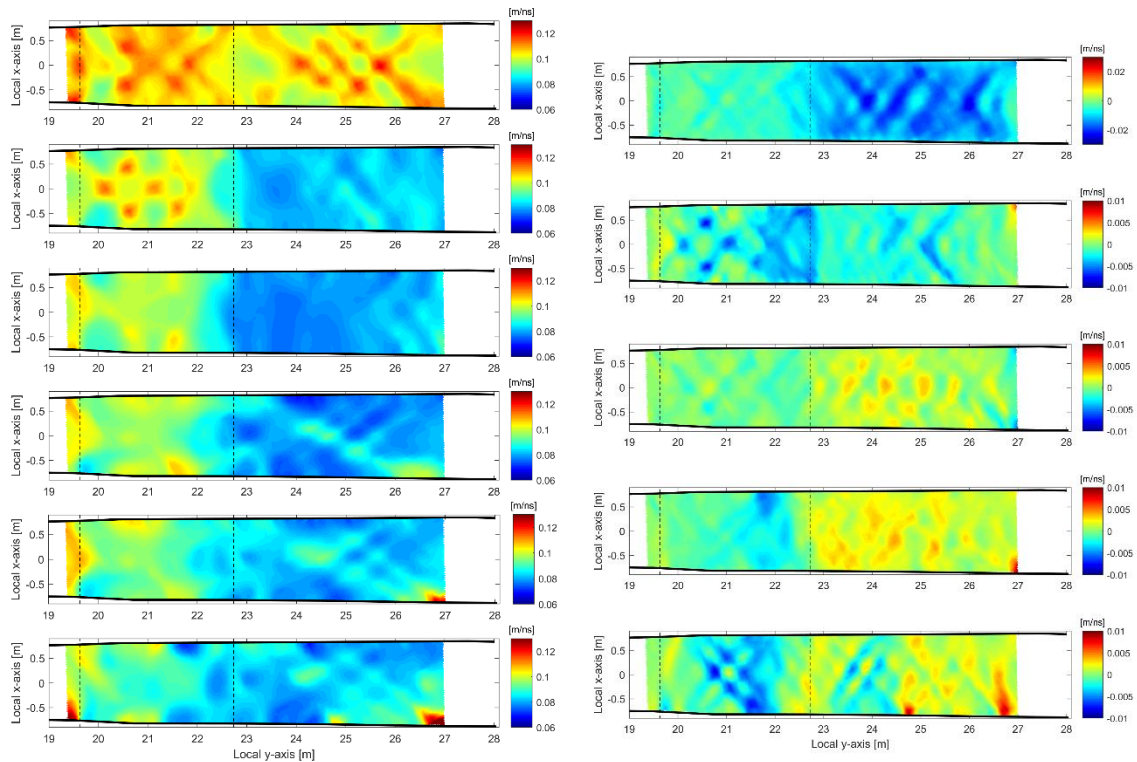
Figure 4. Results from crosshole radar tomography. Left panels show absolute tomograms, and right panels show double-difference tomography results (differences of consecutive experiments).

4. Anomaly detection algorithms

Geophysical tomography often requires extensive data analyses and substantial computer resources. Therefore, it was checked, if it is possible to employ quick and inexpensive tools, with which temporal changes in a repository can be detected, but not necessarily imaged. For that purpose, an anomaly detection algorithm has been developed.

The methodology is based on the idea to use computer vision techniques to describe the structures in the geophysical data and detect anomalies using feature vectors and direct inversion [11]. The original algorithm was implemented for the gravity field data, and it was tested on a predefined set of simple anomaly bodies with density contrasts.

The application to seismic data sets required the algorithm to be modified. As the underlying physical model in seismic phenomena is more complex compared with gravity, it was decided to focus on the supervised learning based on decision trees and support vector machines.

The heart of the modified algorithm is a pre-trained classifier with ability to distinguish predefined normal and abnormal repository configurations. The algorithm itself was updated using synthetic seismic data. The model was simulating an experimental analogue of the repository tunnel with different levels of water saturation. The configuration with low water saturation was selected as an abnormal situation and corresponding data sets were labeled as abnormal, the rest of the data were labeled as normal.

The input data model included 113 sources and 108 receivers. The waveforms of each shot gather was represented as a matrix. The matrices were normalized to a value range from the interval <0,1> and thresholded at 9 levels from 0.1 to 0.9 yielding 9 images.

The seismic velocity and elasticity parameters in the saturated tunnel are so close to those of the host rock, such that the tunnel is nearly invisible. The dry tunnel exhibits more contrast - the reflection of the waves in the tunnel are visible in the thresholded images. The images were converted into feature vectors of the form $[N_{01}, \ldots, N_{09}, S_{01}, S_{02}, \ldots, S_{09}]$ (N_{0n} is the number of objects detected at the threshold level n and S_{0n} is the total area of the objects detected at the corresponding threshold level).

To select the most suitable architecture of the classifier, the Matlab Classification Learner was used to identify the best fitting classifier structure. The best results were obtained with the fine decision tree using the Gini diversity index and maximum number of splits was set to 100. Table 1 summarizes the accuracy of the classification for different classifier types.

Classifier type	Fine tree	Medium tree	Coarse tree	SVN linear	SVN quadratic	SVN cubic	SVN Gaussian
Detailed Description	Max 100 splits	Max 20 splits	Max 5 splits	Linear kernel	Quadratic kernel	Cubic kernel	Gaussian kernel, scale 0.75
General accuracy of classification	87,3 %	85,5 %	82,9 %	77,8 %	81,1 %	86,9 %	87,7 %

Table 1: The different classifier structures and accuracy of the classification

The best results were obtained with the fine decision tree and the SVN based on a fine Gaussian kernel. The abnormal situation in the repository ("dry tunnel") was correctly detected in 91 % of all the simulations using the fine decision tree and in 92 % of all the cases using the SVN structure. In a next step, we implemented the algorithms with the support of Tensor Flow and its libraries. We have trained the decision tree classifier with the same training data as in the Matlab environment. The average classifier accuracy of our implementation was 88 %. The full algorithm is now available in Python.

5.   Geoelectric and induced polarization tomography

ERT is a widely proven and robust method for characterizing subsurface structures and monitoring subsurface processes for geological, geotechnical, hydrological and environmental applications. Recent advancements in data collection hardware and imaging software enabled ERT to become practical for variable scale 3D characterization and high-resolution 4D time-lapse monitoring applications. The sensitivity of subsurface electrical conductivity to a number of important hydrological and geotechnical parameters enables ERT efficiently to provide non-destructive and often non-intrusive information.

Induced polarization (IP) measurements and induced polarization tomography (IPT) can be carried out in parallel to geoelectrical measurements. They are sensitive to additional electrical parameters,

such as chargeability. Low-frequency (below 1 kHz) induced polarization is caused by the transport and accumulation of charge carriers (ions and electrons) in micro-heterogeneous materials (e.g., rock or soil) due to an external electric field. Induced polarization phenomena can be observed both in time and in the frequency domain.

ERT and IPT data are particularly interesting for monitoring bentonite, in which high-level radioactive waste is typically embedded. The electrical conductivity of compacted bentonite blocks and bentonite pellets is influenced by the porosity, dry unit weight, pore water (gravimetric water content, degree of saturation and volumetric water content), as well as pore water salinity. It is found that for high water salinities, the electrical conductivity is most significantly related to the volumetric water content. The high electrical conductivity of injected salt solution has only little effect on changes of the bulk resistivity of the bentonite blocks or pellets on the water contents between 30 and 80 % [12].

We have developed time-lapse (4D) inversion and conceptualization processes with and without petrophysical and thermo-hydro-chemical constraints. Furthermore, measuring and signal processing protocols for simultaneous ERT and IPT imaging of the canister-buffer-bedrock systems were established. Simultaneous inversions of ERT and IPT data allow application of the same geological (structural) constraints to both data sets, thereby enhancing the reliability of the results. The inversion algorithms were tested with a laboratory experiment. First results are encouraging, and it is envisaged to apply the methodology to data sets acquired with a realistic repository monitoring geometry.

6. Calibration and validation of constitutive relationships between electrical parameters and temperature and volumetric water content

For the operational monitoring phase of buffer materials in deep geological repository, saturation and temperature are two key parameters that have been mentioned in every international collaborative work on monitoring strategies and parameters selection. Geoelectrical and induced polarisation data are sensitive to changes in saturation and temperature [13–15]. If a constitutive relationship between the geoelectrical/induced polarisation data and saturation and temperature can be established, this will offer powerful means for non-invasive monitoring of engineered barriers.

For establishing a relationship between geeolectrical/induced polarisation data and saturation and temperature, comprehensive laboratory measurements on bentonite samples were carried out. They were prepared by mechanically mixing bentonite clay with synthetic water up to the target gravimetric water content at 1000 rpm for 5 minutes. All samples were left in a sealed bag for 24 h for homogenization before any test was performed.

The volumetric water content and temperature of the samples was varied systematically, while measuring the electrical resistance and induced polarisation effects. The data were acquired by injecting the current into copper electrodes located at both extremes of the sampler in contact with the cross section of the sample and the difference in potential generated are read by two electrodes located on the top of the sample.

Figure 5 shows the electrical resistivity as a function of volumetric water content and temperature. Resistivity values of the bentonite samples are relatively low, even in samples with low volumetric water content. This was expected, given the good conductivity property of the bentonite material.

As expected, resistivity values decrease with increase of volumetric water content, and there is a decrease of resistivity values with increase of temperature of exposure. Those differences are becoming less pronounced with increasing volumetric water content.

The relationship between volumetric water content, temperature and chargeability is harder to assess (Figure 6). It can be observed that for all temperature series the peak chargeability values are reached between 30 and 50% of volumetric water content. This behaviour may be explained by the presence of fixed sites on the clay surface that are responsible for active IP. When only a few of these sites are occupied by water, there are only a few mobile ions, as they are closely attached to the clay surface, as a result the IP response is small. However, as the volumetric water content increases, the sites become available for ion exchange, which gives a marked increase in the IP response.
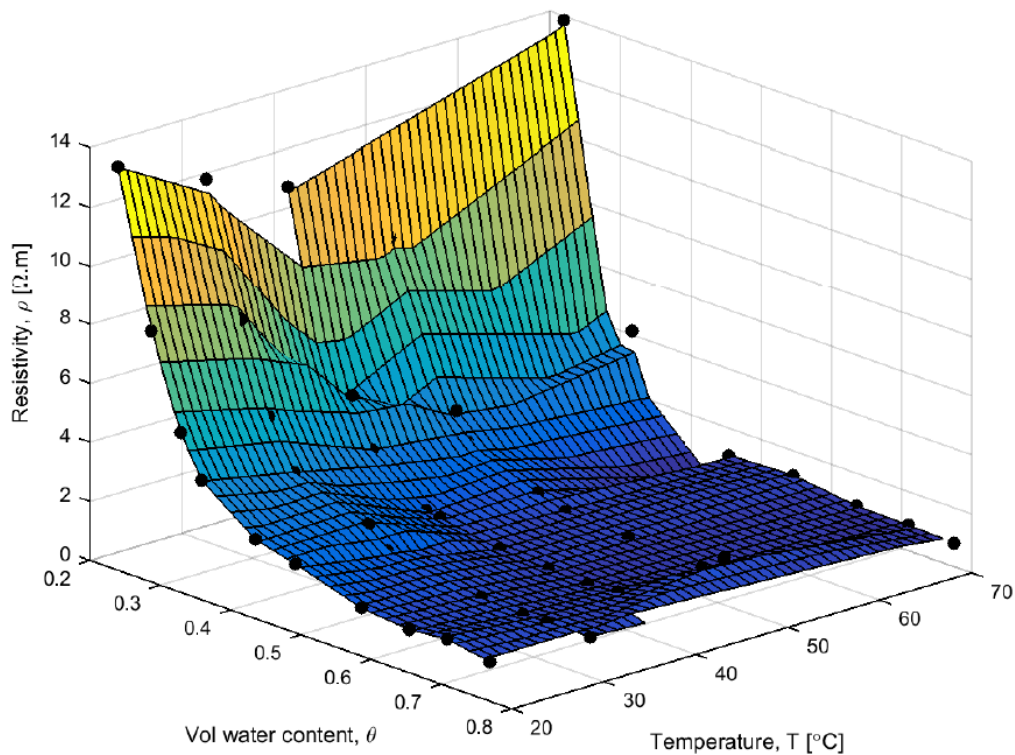

Figure 5. Resistivity results of bentonite samples. Black dots indicate measurements.
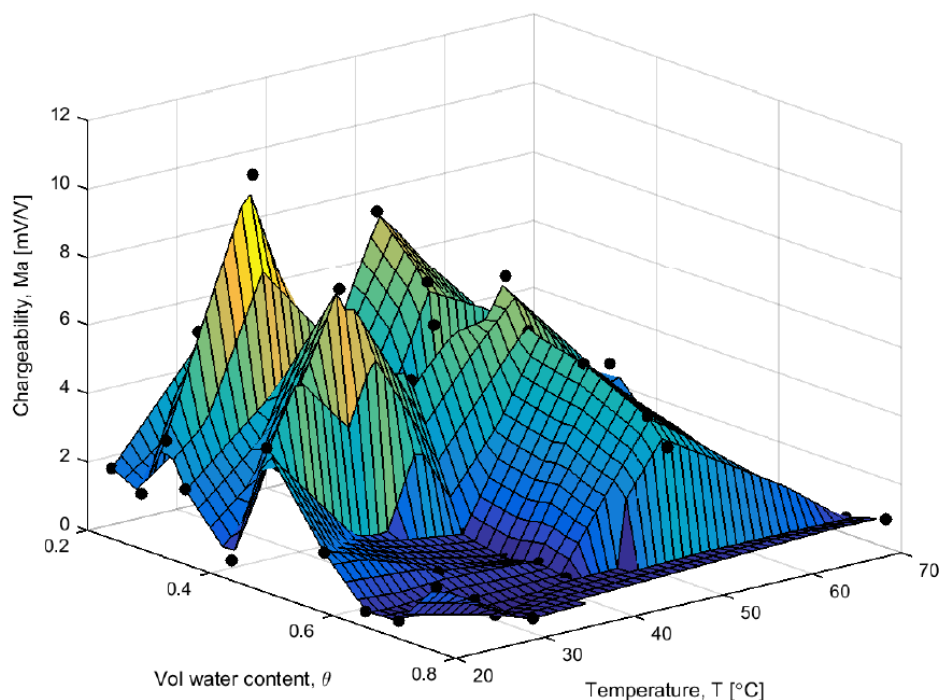
Figure 6. Chargeability results of bentonite samples. Black dots indicate measurements.

7. Conclusions and outlook

In the framework of these studies, several significant advances in geophysical monitoring of high-level radioactive waste repositories could be achieved. Key developments can be summarized as follows.

- *Seismic full waveform inversion (FWI)*
  - o The long-standing problem of FWI in the presence of anisotropy could be solved using a novel parameterization scheme and structural constraints.
  - o The method was validated with an application to a realistic field data set.
- *Differential tomography*
  - o Novel procedures for performing differential inversions have been developped.
  - o The methods were validated with an application to a crosshole radar data set, but it is important to note that this technology can be transferred easily to other inversion problems, such as FWI and ERT/IPT.
- *Anomaly detection*
  - o An anomaly detection algorithm, suitable for seismic data, has been proposed. Initial tests with synthetic data are promising.
- *Geoelectrical and induced polarization tomography (ERT/IPT)*
  - o Suitable algorithms for inverting geoelctrical and induced polarization data have been implemented.
  - o They were validated with laboratory-scale experiments.
- *Calibration of geoelectrical and induced polarization data*

      o Constitutive relationships between geoelectrical/induced polarization data and volumetric water content and temperarture have been established using comprehensive laboratory tests.

Despite the various successes, further research is required for making these technologies applicable for actual repository monitoring. Important tasks that are already scheduled include

- application of the newly developed differential tomography algorithm to FWI problems,
- validation of the anomaly detection algorithm with field data, and
- larger-scale geoelectrical investigations at the Tournemire test site.

5. Acknowledgements

References

1. T. Alkhalifah & R.-É. Plessix, A recipe for practical full-waveform inversion in anisotropic media: An analytical parameter resolution study. *Geophysics*, **79** (2014) R91–R101. https://doi.org/10.1190/geo2013-0366.1.
2. Y. Gholami, R. Brossier, S. Operto, A. Ribodetti, & J. Virieux, Which parameterization is suitable for acoustic vertical transverse isotropic full waveform inversion? Part 1: Sensitivity and trade-off analysis. *Geophysics*, **78** (2013) R81–R105. https://doi.org/10.1190/geo2012-0204.1.
3. A. Guitton & T. Alkhalifah, A parameterization study for elastic VTI full-waveform inversion of hydrophone components: Synthetic and North Sea field data examples. *Geophysics*, **82** (2017) R299–R308. https://doi.org/10.1190/geo2017-0073.1.
4. E. Manukyan & H. Maurer, Imaging of radioactive waste repository with vertically transversely isotropic full waveform inversion VTI FWI for radioactive waste repository imaging. (2018) 4743–4747.
5. G. W. Lanyon, *HG-A (gas path through host rock and along seals) experiment: Discrete Fracture Network Models of Excavation Damage Zone at the HG-A site* (2008).
6. J. Doetsch, N. Linde, & A. Binley, Structural joint inversion of time-lapse crosshole ERT and GPR traveltime data. *Geophysical Research Letters*, (2010). https://doi.org/10.1029/2010GL045482.
7. C. Hauck & D. V Muhll, Permafrost monitoring using time-lapse resistivity tomography. *Permafrost, Vols 1 and 2*, (2003).
8. E. Manukyan, H. Maurer, S. Marelli, S. A. Greenhalgh, & A. G. Green, Seismic monitoring of radioactive waste repositories. *Geophysics*, **77** (2012) EN73-EN83. https://doi.org/10.1190/geo2011-0420.1.
9. A. Asnaashari, R. Brossier, S. Garambois, F. Audebert, P. Thore, & J. Virieux, Time-lapse seismic imaging using regularized full-waveform inversion with a prior model: Which strategy? *Geophysical Prospecting*, (2015). https://doi.org/10.1111/1365-2478.12176.
10. H. R. Müller, B. Garitte, T. Vogt, S. Köhler, T. Sakaki, H. Weber, T. Spillmann, M. Hertrich, J. K. Becker, N. Giroud, V. Cloet, N. Diomidis, & T. Vietor, Implementation of the full-scale emplacement (FE) experiment at the Mont Terri rock laboratory. *Swiss Journal of Geosciences*, (2017). https://doi.org/10.1007/s00015-016-0251-2.

11.   L. Kosková & J. Novák, Application of Edge and Line Detection to Detect the near Surface Anomalies in Potential Data. (2012) 693–696. https://doi.org/10.5220/0004261206930696.

12.   S. Rahimi & S. Siddiqua, Relationships between Degree of Saturation, Total Suction, and Electrical and Thermal Resistivity of Highly Compacted Bentonite. *Journal of Hazardous, Toxic, and Radioactive Waste*, (2018). https://doi.org/10.1061/(ASCE)HZ.2153-5515.0000380.

13.   P. Cosenza, A. Ghorbani, N. Florsch, & A. Revil, Effects of drying on the low-frequency electrical properties of Tournemire argillites. *Pure and Applied Geophysics*, **164** (2007) 2043–2066. https://doi.org/10.1007/s00024-007-0253-0.

14.   T. Hermans, S. Wildemeersch, P. Jamin, P. Orban, S. Brouyère, A. Dassargues, & F. Nguyen, Quantitative temperature monitoring of a heat tracing experiment using cross-borehole ERT. *Geothermics*, **53** (2015) 14–26. https://doi.org/10.1016/j.geothermics.2014.03.013.

15.   A. J. Merritt, J. E. Chambers, P. B. Wilkinson, L. J. West, W. Murphy, D. Gunn, & S. Uhlemann, Measurement and modelling of moisture-electrical resistivity relationship of fine-grained unsaturated soils and electrical anisotropy. *Journal of Applied Geophysics*, **124** (2016) 155–165. https://doi.org/10.1016/j.jappgeo.2015.11.005.